ABMP update

S. Alekhin[1], M.V. Garzelli[2,1], S.-O. Moch[1], O. Zenaiev[1],

[1] II Institut für Theoretische Physik, Universität Hamburg
[2] CERN, Theory Department

Mainly on the basis of [arXiv:2407.00545[hep-ph]]
and work in progress.

PDF4LHC 2024 meeting, December 2nd-3rd, 2024

Heavy-quark pair hadroproduction in QCD and fits of SM quantities

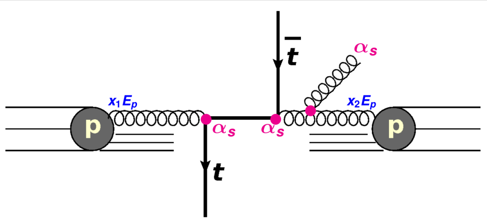

- m_t, $\alpha_s(M_Z)$, g, q and $\bar{q}$ PDFs are inputs for the computation of $pp \to t\bar{t} + X$ cross sections already at LO.
- m_t, q and $\bar{q}$ PDFs also appear in the computation of cross sections for single-top production at LO, whereas in the *s*- and *t*-channels the dependence on $\alpha_s(M_Z)$ and g PDFs appear only at higher orders.

$\Rightarrow$ If we want to use the cross-section data to extract PDFs, we have to take into account the correlations with m_t and $\alpha_s(M_Z)$ (unless one supposes to know already the values of m_t and $\alpha_s(M_Z)$, e.g. from independent measurements).

$\Rightarrow$ Simultaneous fits of PDFs, $m_t(m_t)$ and $\alpha_s(M_Z)$ have been performed:
- ABMP16, using total inclusive top data [S. Alekhin et al., PRD 96 (2017) 014011],
- ABMPtt, using multidifferential top data $\to$ this talk.

x intervals probed by $t\bar{t} + X$ hadroproduction

- $pp \to t\bar{t} + X$ @ 13 TeV probes $0.002 \lesssim x \lesssim 0.7$
  - gg contributes $\approx 90\%$
- (double)-differential data probe different x subintervals
- in particular we consider distributions double-differential in $M(t\bar{t})$ and $y(t\bar{t})$.
- Scales m_H, M_W, M_Z and m_t are similar among each other
- Higgs production at the LHC probes $x \sim m_H/\sqrt{s} \sim 0.01$ which is well covered by differential $t\bar{t} + X$ data
- DY production at the LHC probes a similar region $x \sim m_{W,Z}/\sqrt{s}$
  - mostly sensitive to quark PDFs
  - helps with light flavor separation

LO: $x_{1,2} = (M(t\bar{t})/\sqrt{s}) \exp[\pm y(t\bar{t})]$

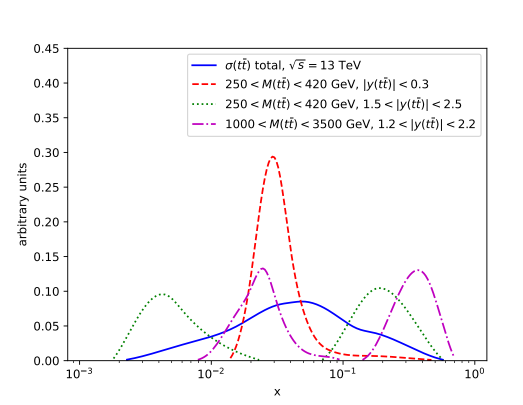

Our theory calculations with MATRIX + PineAPPL framework

- NNLO computations for total and multi-differential $pp \to t\bar{t} + X$ cross sections can now be performed thanks to the publicly available MATRIX framework [Catani, Devoto, Grazzini, Kallweit, Mazzitelli Phys.Rev.D 99 (2019) 5, 051501; JHEP 07 (2019) 100]
  - fully differential NNLO calculations were also published in JHEP 04 (2017) 071 [Czakon, Heymes, Mitov] , but no public code available. However, the HighTEA database [Czakon et al., arXiv:2304.05993] has recently appeared.
- We use private version of MATRIX [Grazzini, Kallweit, Wiesemann, EPJC 78 (2018) 537]
- Interfaced to PineAPPL [Carrazza at al., JHEP 12 (2020) 108] to produce interpolation grids which are further used in xFitter https://gitlab.com/fitters/xfitter
  - reproduce NNLO calculations using any PDF + $\alpha_s(M_Z)$ set and/or varied μ_r, μ_f in $\sim$ seconds
  - interface implemented privately and only for the $pp \to t\bar{t} + X$ process
- Further modifications to MATRIX to make possible runs with $\Delta\sigma_{t\bar{t}} < 0.1\%$
  - adapted to DESY Bird Condor cluster and local multicore machines
  - technical fixes related to memory and disk space usage, etc.
- We did runs with different m_t values with step of 2.5 GeV and $\Delta\sigma_{t\bar{t}} = 0.02\%$
  - $\approx$ 350000 CPU hours/run ($\sim$30 years on a single CPU)
  - for differential distributions, statistical uncertainties in bins are $\lesssim 0.5\%$
- $\mu_r = \mu_f = H_T/4$, $H_T = \sqrt{m_t^2 + p_T^2(t)} + \sqrt{m_t^2 + p_T^2(\bar{t})}$, varied up and down by factor 2 with $0.5 \leq \mu_r/\mu_f \leq 2$ (7-point variation)

ATLAS and CMS data used in this work

- We focus especially on measurements at 13 TeV where double-differential $M(t\bar{t})$, $y(t\bar{t})$ cross sections at parton level are available
  - **(1)** CMS EPJ C80 (2020) 658 [1904.05237, TOP-18-004]:
    2D cross sections in dileptonic channel, $L = 35.9\ \text{pb}^{-1}$
    - for 3D $M(t\bar{t})$, $y(t\bar{t})$, N_{jet} cross sections, NNLO is not available for $t\bar{t}$ + jets + X
  - **(2)** CMS Phys.Rev.D104 (2021) 9, 092013 [2108.02803, TOP-20-001]:
    2D cross sections in l+jets channel, $L = 137\ \text{pb}^{-1}$
  - **(3)** ATLAS EPJ C79 (2019) 1028 [1908.07305]:
    2D cross sections in l+jets channel, $L = 36\ \text{pb}^{-1}$
  - **(4)** ATLAS JHEP 01 (2021) 033 [2006.09274]:
    2D cross sections in all-hadronic channel, $L = 36.1\ \text{pb}^{-1}$
- For all measurements, we use normalised cross sections unfolded to the final-state parton level
- We use information on correlations of experimental uncertainties as provided in the paper (1) or in the HEPDATA database (2,3,4)
  - assumed no correlation between different measurements
    (reasonable assumption for normalised cross sections)
- it would be interesting to also add LHCb data (sensitivity to larger x and to m_t), but they are only available in the fiducial phase-space (cuts on leptons)
- Additionally, we use total inclusive $t\bar{t} + X$ and single-top cross-section data at all energies, according to summary plots by the LHC Top Working Group + Tevatron.

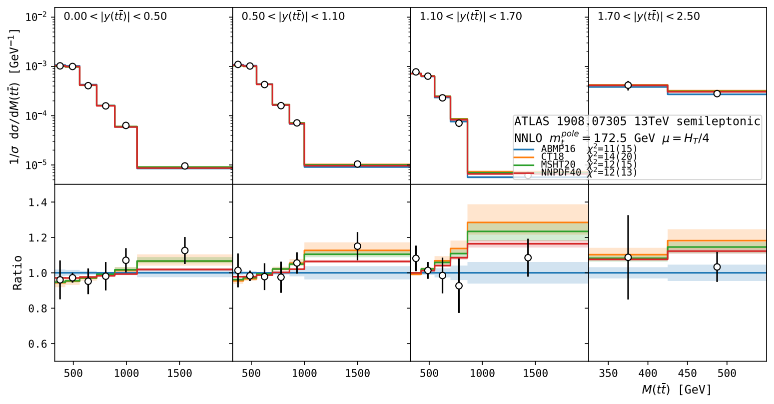

- Fixed $m_t^{\text{pole}} = 172.5$ GeV, $\mu_r = \mu_f = H_T/4$
- Reported χ^2 values with (and without) PDF uncertainties
- All PDF sets describe data equally well
- $\chi^2/\text{dof} < 1$ indicating possible overestimate of experimental uncertainties (additionally, the data covariance matrix is not singular, i.e. $\det(\text{cov}) \neq 0$: we suspect this is related to numerical inaccuracy of data stored in Hepdata. This affects estimates of correlated uncertainties. Same issue in the $\sqrt{s} = 8$TeV ATLAS analysis [arXiv:1607.07281].

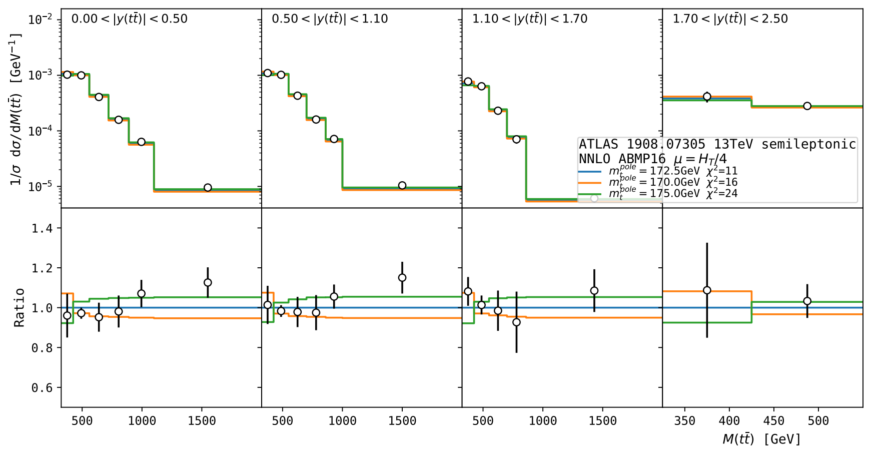

- Using ABMP16, $\mu_r = \mu_f = H_T/4$
- Reported χ^2 values with PDF uncertainties
- Large sensitivity to m_t^{pole} in the first $M(t\bar{t})$ bin (and even in other $M(t\bar{t})$ bins, thanks to cross section normalisation). The sensitivity does not increase with rapidity due to cross-section normalization.

Pulls of ATLAS 1908.07305 data with respect to ABMP predictions

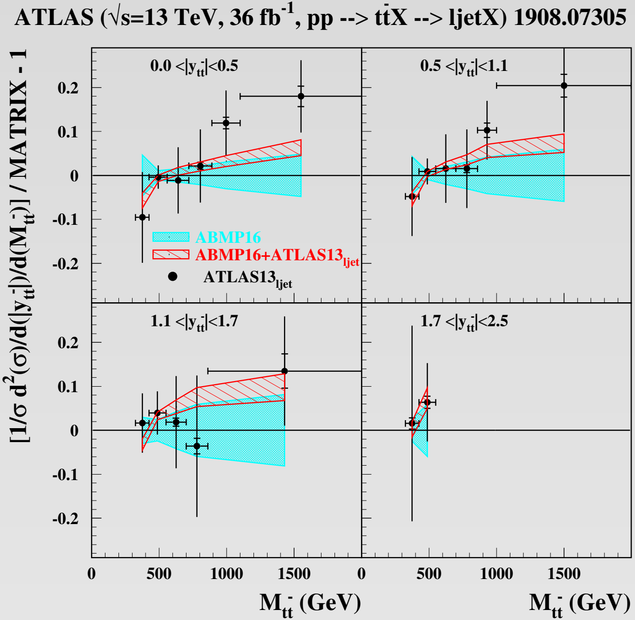

- ABMP PDF fit variant incorporating this specific dataset, w.r.t. already available ABMP16 PDF fit without it.
- ATLAS $\ell + j$ data tend to be larger than central theory predictions at large $M(t\bar{t}) \sim 1500$ GeV. But the data uncertainties are still large.
- ATLAS $\ell + j$ analysis with better statistics wanted.

Pulls of ATLAS 2006.09274 data with respect to ABMP predictions

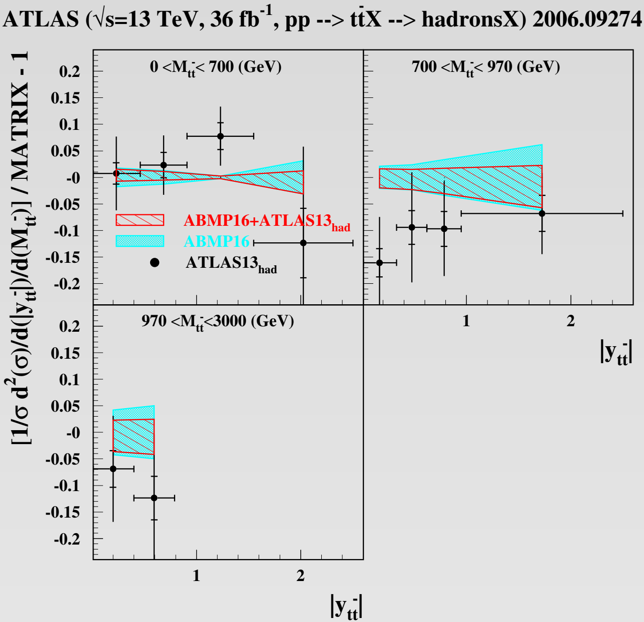

- ABMP PDF fit variant incorporating this specific dataset, w.r.t. already available ABMP16 PDF fit without it
- ATLAS hadronic data smaller than central theory predictions at large $M(t\bar{t})$.
- ATLAS $(\ell + j)$ data larger than central theory predictions at large $M(t\bar{t})$.

CMS TOP-20-001 vs NNLO predictions

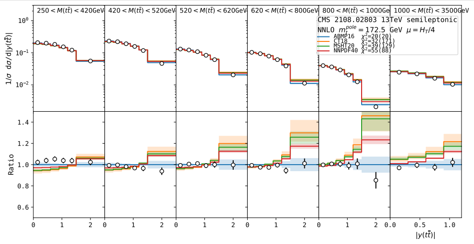

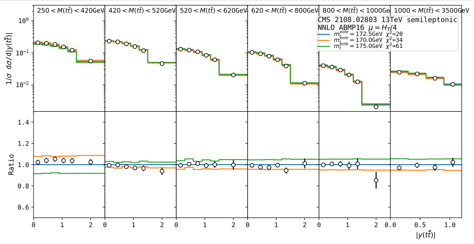

- $\mu_r = \mu_f = H_T/4$
- Reported χ^2 values with (and without) PDF uncertainties
- All PDF sets describe data reasonably well, with best description by ABMP16
  - CT18, MSHT20 and NNPDF40 show clear trend w.r.t data at high $y(t\bar{t})$ (large x)
- This is most precise currently available dataset with finest bins

Pulls of CMS TOP-20-001 data with respect to ABMP predictions

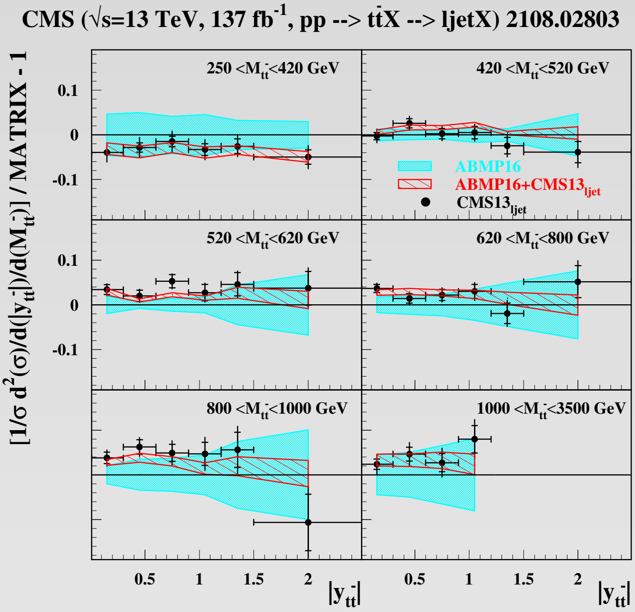

- ABMP PDF fit variant incorporating this specific dataset, w.r.t. already available ABMP16 PDF fit without it

Pulls of CMS TOP-18-004 data with respect to ABMP predictions

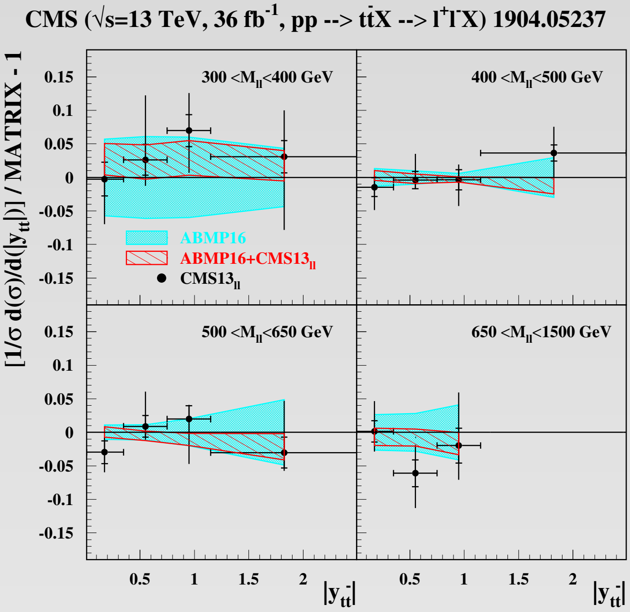

- ABMP PDF fit variant incorporating this specific dataset, w.r.t. already available ABMP16 PDF fit without it

Partial χ^2 for variants of the new ABMP analysis including double-differential $t\bar{t} + X$ data at 13 TeV

Experiment	Dataset	$\sqrt{s}$ (TeV)	NDP	χ^2		
				I	II	III
ATLAS	ATLAS13$_{ljet}$	13	19	34.0	28.2	–
	ATLAS13$_{had}$	13	10	11.9	11.6	–
CMS	CMS13$_{ll}$	13	15	20.7	–	19.6
	CMS13$_{ljet}$	13	34	44.3	–	42.4

Table: The values of χ^2 obtained for various $t\bar{t} + X$ datasets included in the present analysis (column I: both ATLAS and CMS datasets; column II: only ATLAS ones; column III: only CMS ones).

- In comparison to the fit including both CMS datasets (III), the χ^2 slightly deteriorates when including also the datasets of the ATLAS analyses (I), but is still compatible within statistical uncertainties.
- In comparison to the fit including both ATLAS datasets (II), the χ^2 for the all-hadronic dataset remains compatible within statistical uncertainties when including also the datasets of the CMS analysis (I). Viceversa the χ^2 for the ATLAS $\ell + j$ dataset worsens. $\Rightarrow$ Tension of the ATLAS $\ell + j$ dataset with all other datasets

Extracted $g(x)$ in variants of the ABMP fit

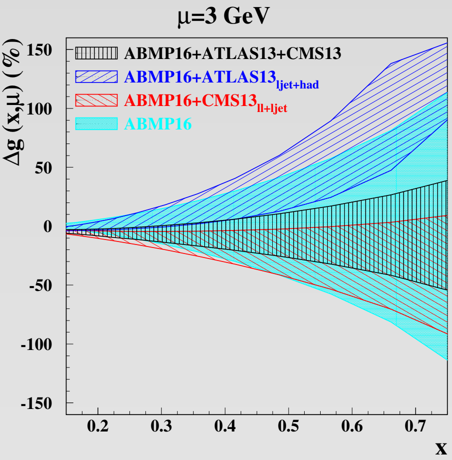

- $g(x)$ at the starting scale $\mu = 3$ GeV.
- $g(x)$ in the new ABMP fit variants compatible with ABMP16 previous fit.
- uncertainties on $g(x)$ decreased by a factor ~ 2 w.r.t. ABMP16 previous fit.
- ATLAS and CMS data points towards opposite trends of $g(x)$ at large x. ATLAS prefers a larger $g(x)$, related to the fact that ATLAS $(\ell + j)$ data tend to be larger than theory predictions at large $M(t\bar{t}) \sim 1500$ GeV. Note that this trend is not visible for ATLAS hadronic data.
- fit including both ATLAS and CMS data dominated by the CMS $\ell + j$ differential data.
- Observe that new $m_t(m_t)$ and $\alpha_s(M_Z)$ values are extracted simultaneously. In particular, the smaller $g(x)$ of the “global” fit is accompanied by a smaller $m_t(m_t)$ value (see next slides).

Extracted values of $m_t(m_t)$ in variants of the ABMP fit

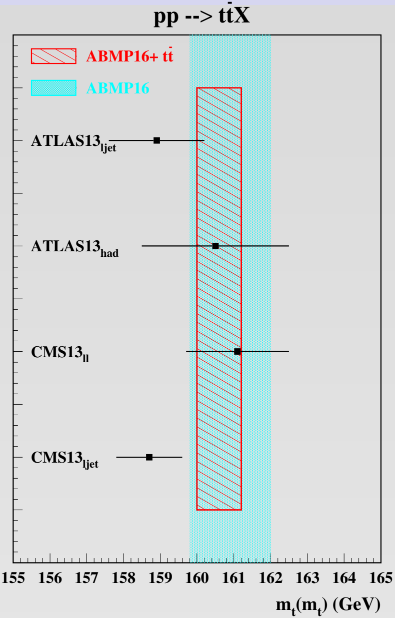

- Legenda:
  Black: ABMP PDF fit variant incorporating a single specific dataset,
  light-blue: previous ABMP16 PDF fit,
  red: new ABMP PDF fit, incorporating all $t\bar{t} + X$ double-differential data at 13 TeV.

- Good compatibility of $m_t(m_t)$ extracted in the different variants of the fit.
- ATLAS hadronic data are too uncertain to play a constraining role on $m_t(m_t)$.
- New central value of $m_t(m_t)$ = 160.6 GeV slightly smaller than 160.9 GeV obtained in the previous ABMP16 fit, due to effect of the ATLAS and CMS $\ell + j$ differential data.
- Including all 13 TeV $t\bar{t} + X$ double-differential data allow to decrease by a factor 2 the uncertainty band on $m_t(m_t)$, varying from 1.1 GeV to 0.6 GeV.
- Observe that new PDFs and $\alpha_s(M_Z)$ values are extracted simultaneously.

Correlation between $m_t(m_t)$ and $\alpha_s(M_Z)$ in the new ABMP fit (vs. old ABMP16)

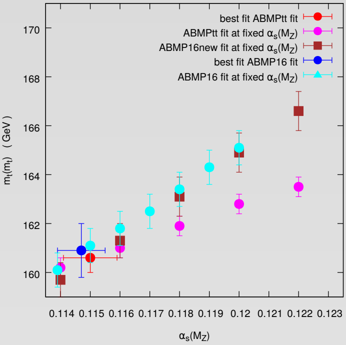

$\alpha_s(M_Z, N_f = 5)$		$m_t(m_t)$ (GeV)
Fitted	0.1150(9)	160.6(6)
$\alpha_s(M_z)$ fixed	0.114	160.2(4)
	0.116	161.0(4)
	0.118	161.9(4)
	0.120	162.8(4)
	0.122	163.5(4)

Table: The values of $m_t(m_t)$ obtained with different values of α_s in the new ABMP fit.

- Correlations between PDF $g(x)$, $\alpha_s(M_Z)$ and $m_t(m_t)$ follows from the factorization theorem.
- Fit of $m_t(m_t)$ at fixed $\alpha_s(M_Z)$ shows positive correlation between $\alpha_s(M_Z)$ value and $m_t(m_t)$.
- When including the $t\bar{t} + X$ differential data, the correlation coefficient decreases w.r.t. to the ABMP16 analysis, whereas the best-fit $\alpha_s(M_z)$ value remains approximately the same.
- With improved precision of data on single-top production in the t-channel, the impact of $\alpha_s(M_Z)$ on the m_t determination could be further leveled.

Extracted $g(x)$ in comparison with global PDF fits

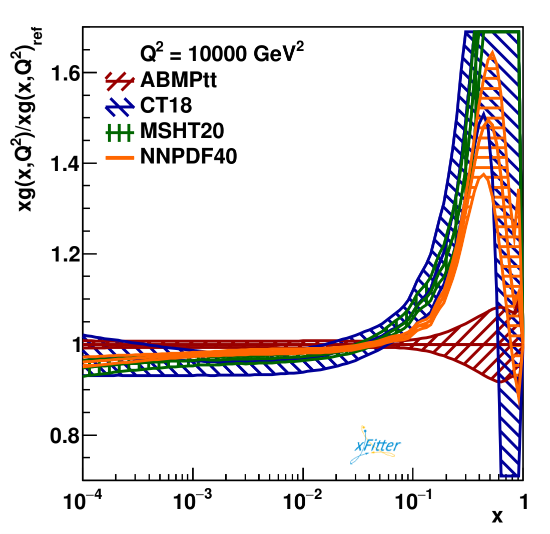

$*$ Large differences at large x: Besides the effect of the $t\bar{t} + X$ data, these are due to different $\alpha_s(M_Z)$ treatment, heavy-flavour DIS scheme, etc.

PDF fits using as input different $\alpha_s(M_Z)$ values

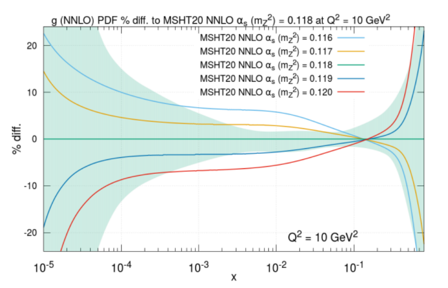

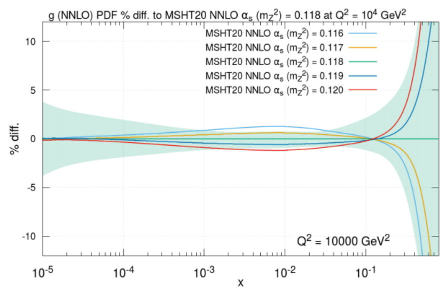

from T. Cridge et al., MSHT20, arXiv:2106.10289

∗ Different $\alpha_s(M_Z)$ values as input play a large impact on the gluon at all x values, especially at small Q^2

$\Rightarrow$ If $\alpha_s(M_Z)$ in MSHT20 would be similar to the one in ABMP16, the $g(x)$ would also look more similar to the latter (at least in the region covered by $t\bar{t}$ data).

$(\alpha_s(M_Z), xg(x,\mu))$ correlation coefficient as a function of x

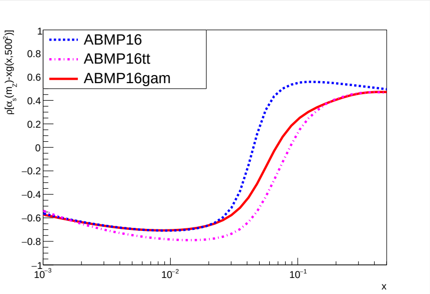

$*$ For $x > 0.1$, for increasing $\alpha_s(M_Z)$, ABMPtt $g(x)$ becomes larger

$*$ For $x < 0.1$, for increasing $\alpha_s(M_Z)$, ABMPtt $g(x)$ becomes smaller

$*$ For $x > 6 \cdot 10^{-2}$ correlations reduced in ABMPtt fit with respect to ABMP16

$*$ Correlations also reduced in the ABMP16gam variant of ABMP16 fit (including updated $t\bar{t} + X$ inclusive cross-section data).

Conclusions from the ABMPtt studies

- Double-differential $M(t\bar{t})$, $y(t\bar{t})$ cross sections included in the ABMPtt PDF + $\alpha_s(M_Z)$ + $m_t(m_t)$ fit make it possible to reduce gluon PDF uncertainties at large x and $m_t(m_t)$ uncertainties by a factor ~ 2 with respect to ABMP16 fit, retaining consistency, with no impact on the $\alpha_s(M_Z)$ value and uncertainty.
- $m_t(m_t)$ fitted value from different variants of the fit agree among each other within uncertainties.
- correlations between $m_t(m_t)$ and $\alpha_s(M_Z)$ reduced by the inclusion of double-differential data in the fit w.r.t. to the case of total cross sections, where the effects of correlations are much larger.
- ATLAS $(\ell + \mathrm{j})$ data characterized by the worst theory description, in tension with all other data. A new ATLAS $(\ell + \mathrm{j})$ analysis producing normalized double-differential distributions with larger statistics (full Run 2 statistics) is needed.
- We encourage combinations of datasets in different channels, of ATLAS and CMS datasets and unfolding to parton-level by LHCb.

Publicly available: grids for NNLO predictions of $t\bar{t} + X$ at the LHC

- We have made public the grids of NNLO QCD predictions we obtained from the `MATRIX + PineAPPL` framework, to facilitate their public use.

  We use the `Ploughshare` web-based utility for the automated distribution of fast interpolation grids for HEP:

  https://ploughshare.web.cern.ch/ploughshare/

  The `Ploughshare` C++ library can be called directly in your program (e.g. in the PineAPPL interface in xFitter), to download the grids.

CMS	pp nnlo	13 TeV	ttbar-mt1650	MATRIX	xFitter	2108.02803	xfitter-cms-ttbar-mt1650-arxiv-2108.02803
CMS	pp nnlo	13 TeV	ttbar-mt1675	MATRIX	xFitter	2108.02803	xfitter-cms-ttbar-mt1675-arxiv-2108.02803
CMS	pp nnlo	13 TeV	ttbar-mt1700	MATRIX	xFitter	2108.02803	xfitter-cms-ttbar-mt1700-arxiv-2108.02803
CMS	pp nnlo	13 TeV	ttbar-mt1725	MATRIX	xFitter	2108.02803	xfitter-cms-ttbar-mt1725-arxiv-2108.02803
CMS	pp nnlo	13 TeV	ttbar-mt1750	MATRIX	xFitter	2108.02803	xfitter-cms-ttbar-mt1750-arxiv-2108.02803
CMS	pp nnlo	13 TeV	ttbar-mt1775	MATRIX	xFitter	2108.02803	xfitter-cms-ttbar-mt1775-arxiv-2108.02803

  Each .tgz file, using as input a different m_t value, includes:
  – grid for double-differential distributions (Run 2) ($\sim$ 1000 MB)
  – grid for single-differential distributions (Run 1) ($\sim$ 250 MB)
  – grid for total cross sections ($\sim$ 5 MB)
  – json file with information on the input used to generate the grids and citations.

  Each grid is in PineAPPL format (.opt):
  bins in $M(tt)$, $y(tt)$; for each bin, grid of components of partonic cross-sections as a function of x_1, x_2, μ_F^2.
  Different components correspond to different α_s powers, $\ln^k \mu_r$, $\ln^l \mu_f$, $ln\mu_r \ln \mu_f$ terms.

$\Rightarrow$ Allows for reconstructing LO, NLO, NNLO distributions with whichever PDFs and $\alpha_s(M_Z)$ and scale variations around the central scale $H_T/4$.

Publicly available

- ABMPtt PDFs in LHAPDF format are available on the web under:
  - `https://lhapdf.hepforge.org/pdfsets.html`

  ABMPtt_3_nnlo: 43500, ABMPtt_4_nnlo: 43530, ABMPtt_5_nnlo: 43560

  Thanks to the support of the LHAPDF team

- Example of predictions one can build from publicly available PDFs and grids:

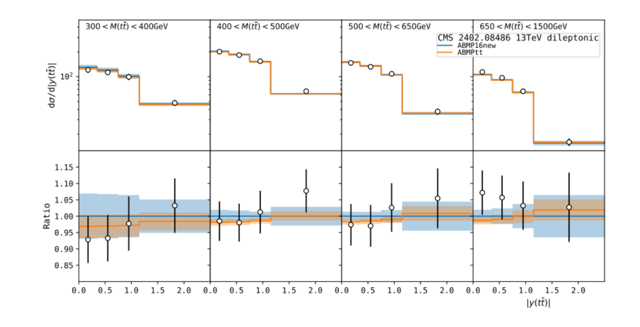

Comparison of ABMPtt predictions with most recent CMS recent $t\bar{t} + X$ data [arXiv:2402.08486], not yet in the fit. How will the fit perform w.r.t. new ATLAS data ?

Photon in fits

Knowing γ content of p is increasingly important at increasing higher orders. Two approaches have been considered so far:

- γ according to the LUXQed approach
  - implemented in most modern PDF fits, basically following the guidelines in the LUXQed papers, with some variations. Photon distributions are computed by first principles, however relying on assumptions/fits concerning the proton structure functions F_2 and F_L down to low scales Q^2 and/or low hadronic invariant mass W^2 and concerning the elastic contributions to F_2 and F_L
- γ treated similarly to partons
  - photon distribution parameterized at a low scale and then evolved
  - initial condition fixed at such a scale (difficult to establish, because the available experimental data are hardly constraining photons at low scales).
  - photon evolves with standard evolution equations (resummation effects included)

  - photon generated radiatively above a given (fitted) scale.
  - supplemented by an elastic component.

  - approaches used in pre-LUXQed PDFs

We are considering the various approaches in the ABMP framework. Selected PRELIMINARY results (LO QED + NNLO QCD evolution) :

- considerations and comparisons of variants of ABMP fit including photons
- tensions among datasets for non-resonant dilepton production

ABMP variants including photon

- LUXQed-style ABMP photon (with some modifications with respect to original LUXQed papers): $\gamma^{inel}(x, \mu^2)$ extracted at each scale μ by the LUXQed integral over inelastic structure functions, with DIS computed using as a basis the ABMP16 fit. $\gamma^{el}(x)$ also extracted.

- ABMP variant with γ generated radiatively above $\mu_0 = 3$ GeV. $\gamma(x, \mu_0 = 3\text{ GeV}) = 0$, LO QED + NNLO QCD evolution. QCD-QED interference effects neglected.
  The presence of photons influences parton distributions according to sum rules.
  γ completely fixed by above conditions.
  Fit of parton distributions (and other quantities) including ABMP16 data (with update on $t\bar{t}$ inclusive cross-section data and on c and b DIS data) + LHC non-resonant dilepton production data

- ABMP distribution with γ parameterized at $\mu_0 = 3$ GeV according to $Ax^\alpha(1 - x)^\beta$.
  Parameters of the initial condition fitted, using LHC non-resonant dilepton production data.

Elastic component γ^{el} of the photon distribution in LUXQed formalism

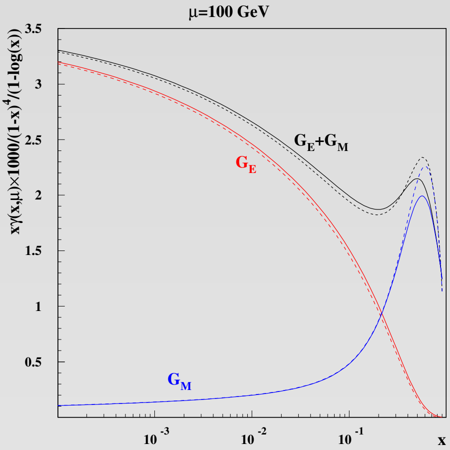

γ^{el} depends on F_2^{el} and F_L^{el}, which, in turn, depend on the electric and magnetic elastic form factors.

Dipole parameterization of the latter good to study asymptotic behaviour,

LUXQed uses A1 fit (2014) up to $x = 0.9$.

We use the Arrington, Hill and Lee fit (2018).

$\Rightarrow$ Non negligible differences at large $x \sim 0.5$.

$F_L^{inel}(x, Q^2)$, contributing to LUXQed γ^{inel}

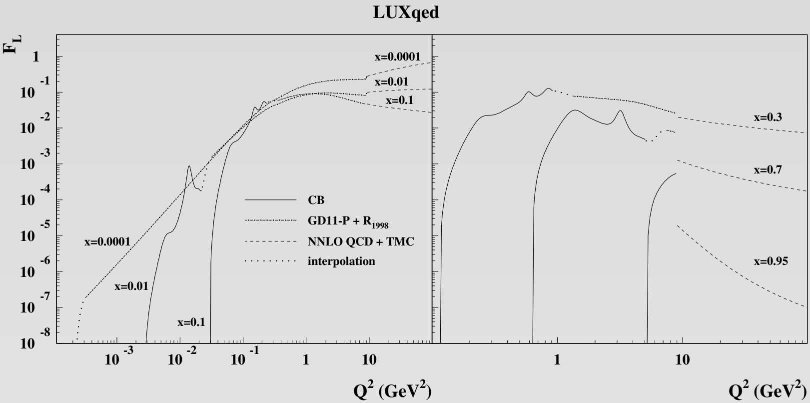

∗ Artificial (forced) separation of the (W^2, Q^2) space in DIS region ($Q^2 > 9$ GeV^2, $W^2 > 4$ GeV^2), ($W^2 < 3$ GeV^2) region and ($Q^2 < 9$ GeV^2, $W^2 > 4$ GeV^2) region.

∗ Discontinuities at the borders between pQCD and non pQCD regions.

Contributions to $\gamma^{inel}(x)$ from the different regions

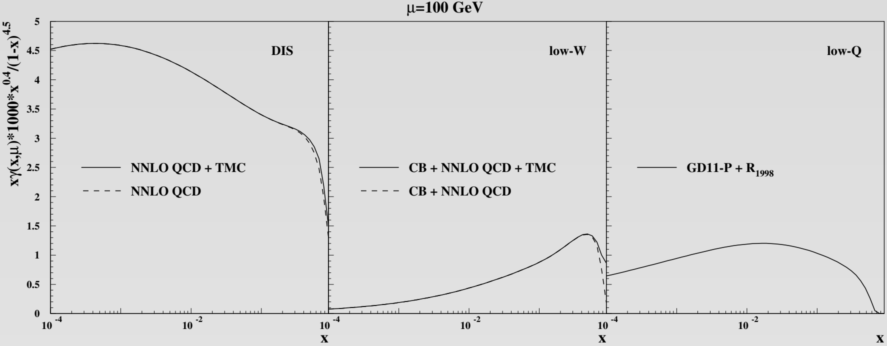

$*$ At large x the contribution from the DIS region drops down, and the one from resonance regions ($W^2 < 3$ GeV^2) becomes increasingly important.

γ distribution as a function of x at fixed $\mu = 100$ GeV: comparison among different approaches/components

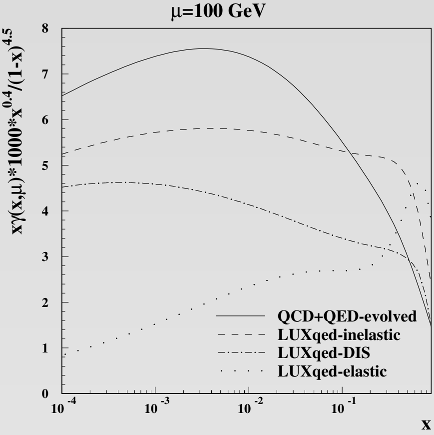

- different shapes of the different LUXQed-ABMP γ components (DIS, etc).
- different shape of the LUXQed-ABMP γ^{DIS} component and the evolved $\gamma(x)$ distribution in the ABMPgam fit variant with $\gamma(\mu = 3 \text{ GeV}) = 0$.

γ distribution as a function of μ for fixed $x = 0.01$: comparison among different approaches/components

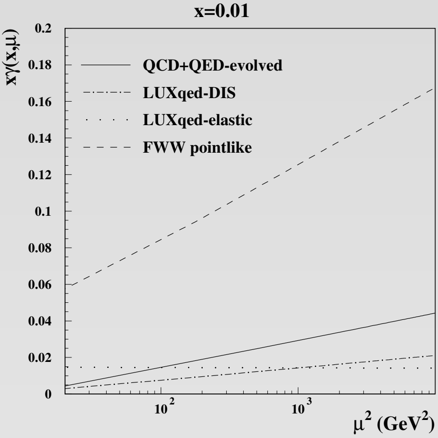

connection between γ distribution and form factors:

- for pointlike FF, γ raises dramatically.
- for elastic FF, LUXQed-ABMP γ^{el} constant.
- the LUXQed-ABMP γ^{DIS} component evolves slowly than the $\gamma(x)$ distribution in the ABMPgam fit variant with $\gamma(\mu = 3$ GeV$) = 0$.

Performances of the ABMPgam fit variant with $\gamma(\mu = 3$ GeV$) = 0$ with respect to CMS experimental data at $\sqrt{S} = 7$ TeV

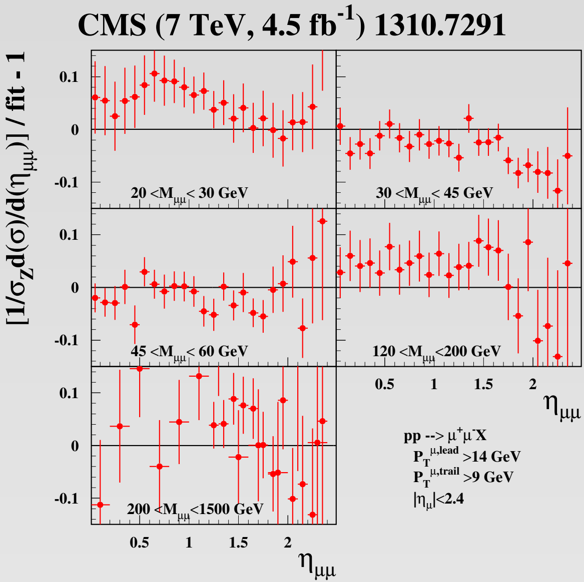

∗ Decent agreement with data in all $M_{\ell^+\ell^-}$ ranges.

Performances of the ABMPgam fit variant with $\gamma(\mu = 3$ GeV$) = 0$ with respect to ATLAS experimental data at $\sqrt{S} = 8$ TeV

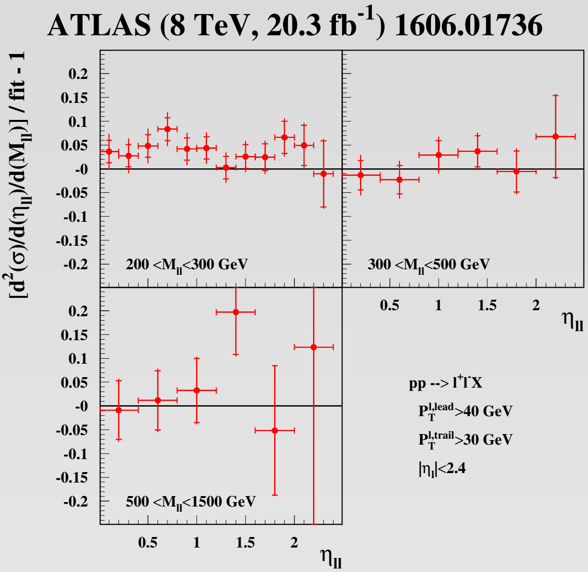

∗ Decent agreement with data at large $M_{\ell^+\ell^-}$

Performances of the ABMPgam fit variant with $\gamma(\mu = 3$ GeV$) = 0$ with respect to ATLAS experimental data at $\sqrt{s} = 8$ TeV

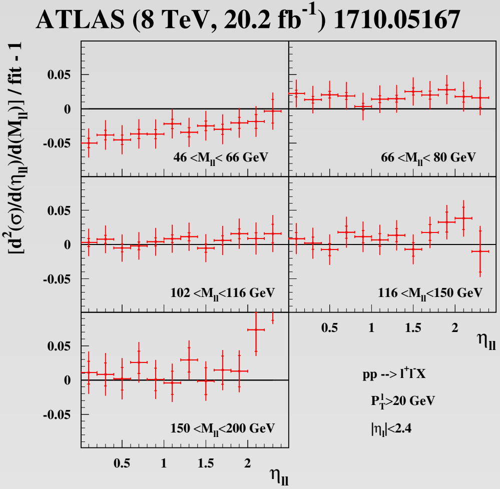

∗ Discrepancies of the order of 2σ in the low $M_{\ell^+\ell^-}$ bins: theory overpredicts data (but compatible within $2\ \sigma$'s)

ABMPgam fit variants with different initial conditions for the photon distribution vs. ATLAS non-resonant dilepton data at $\sqrt{S}$ = 7 TeV

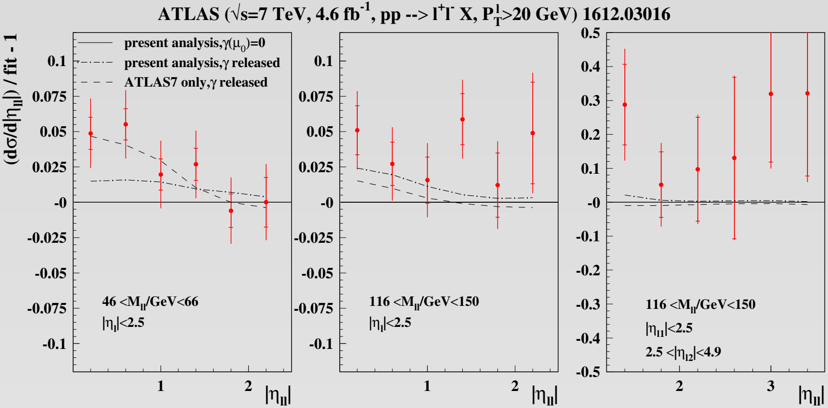

- $\gamma\gamma \to \ell^+\ell^-$ process included in the theory predictions compared to the data.
- The ATLAS data at low ($M_{\ell^+\ell^-}$, $y_{\ell^+\ell^-}$) are in better agreement with central predictions obtained by assuming the presence of a photon component already at the initial starting scale μ_0.
- They are compatible with central predictions with $\gamma(\mu_0) = 0$ within $\sim 2.3\sigma$.

The “bump” in photon distribution

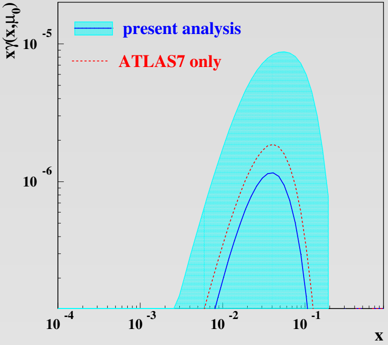

- ATLAS dilepton data at 7 TeV favour the presence of a bump in γ distribution peaked at $x \sim 5 \cdot 10^{-2}$ at the initial scale μ_0. This bump is present both in the variant of the fit without other dilepton data, and, attenuated, in the global fit where the CMS dilepton and other data are also included.
- However ATLAS data, referring to a scale $\mathcal{O}$(100 GeV), are not enough to impose a finite constraint on the γ at scale μ_0. Considering that the CMS data are instead well compatible with an initial condition $\gamma(\mu_0) = 0$, and that data capable of directly constraining photons at such low scales are missing, the uncertainty on the photon in the region of the bump is extremely large.
- We can conclude that the photon in the global ABMPgam fit is compatible with $\gamma(\mu_0) = 0$ at all x values, i.e. with the hypothesis of being generated fully perturbatively. There is no need for an intrinsic photon component at low scales.
- This analysis should be repeated adding other data (e.g. the 13 TeV ones).

$m_t(m_t)$ and $\alpha_s(M_Z)$ in variants of ABMP fits (partly preliminary)

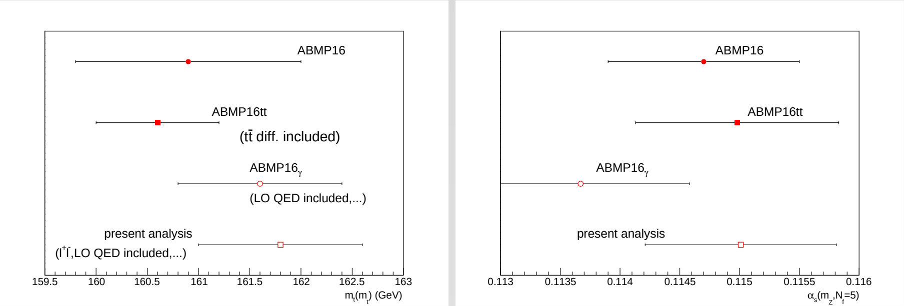

$*$ "ABMP16γ" includes same data as ABMP16 (except single-top), but adds photon generated perturbatively.

$*$ "present analysis", besides photon, adds non-resonant DY data.

$*$ $m_t(m_t)$ values from the four variants all compatible among each other within uncertainties: also true for $m_b(m_b)$ and $m_c(m_c)$

$*$ the $t\bar{t} + X$ differential data play a crucial role in reducing the uncertainties on $m_t(m_t)$, while playing no role on $\alpha_s(M_Z)$.

Main conclusions from ABMPgam PRELIMINARY studies

$*$ Tensions between different datasets for non-resonant dilepton production at the LHC need to be solved.

$*$ LUXQed ABMP γ and γ^{DIS} distributions differ in x and in μ dependence w.r.t. to a radiatively generated photon distribution (with initial condition fixed to $\gamma(x) = 0$ at $\mu_0 = 3$ GeV).

$*$ Datasets at lower scales than LHC data, might be useful for better fitting γ initial condition.

$*$ Even variation of μ_0 needs to be considered.

BACKUP

Theory framework for $t\bar{t} + X$ hadroproduction

- NNLO computations for total inclusive $pp \to t\bar{t} + X$ cross sections can be obtained with theory tools already publicly available since long (`HATHOR`, `Fasttop`, `Top++`).

- NNLO computations for total and multi-differential $pp \to t\bar{t} + X$ cross sections can now be performed thanks to the publicly available `MATRIX` framework [Catani, Devoto, Grazzini, Kallweit, Mazzitelli Phys.Rev.D 99 (2019) 5, 051501; JHEP 07 (2019) 100]
  - fully differential NNLO calculations were also published in JHEP 04 (2017) 071 [Czakon, Heymes, Mitov] , but no public code available. However, the `HighTEA` database [Czakon et al., arXiv:2304.05993] has recently appeared.

- Master formula for $t\bar{t} + X$ hadroproduction in `MATRIX`:

$$d\sigma^{t\bar{t}}_{(N)NLO} = \mathcal{H}^{t\bar{t}}_{(N)NLO} \otimes d\sigma^{t\bar{t}}_{LO} + \left[d\sigma^{t\bar{t}+jet}_{(N)LO} - d\sigma^{t\bar{t},CT}_{(N)NLO} \right]$$

$*$ based on q_T-subtraction for cancelling IR divergences, where $\vec{q}_T = \vec{p}_{t,T} + \vec{p}_{\bar{t},T}$, $\vec{q}_T = 0$ at LO.

$*$ $d\sigma^{t\bar{t}+jet}_{(N)LO}$ is IR divergent for $q_T \to 0$ The counterterm $d\sigma^{t\bar{t},CT}_{(N)NLO}$ compensating for the divergence is known from the fixed-order expansion of the resummation formula of the logarithmic contributions of the form $\alpha_s^{n+2}(1/q_T^2) ln^k(M^2_{t\bar{t}}/q_T^2)$ affecting the q_T distribution, which are large in the limit $q_T \to 0$. $\Rightarrow$ The square bracket is finite for $q_T \to 0$.

$*$ in practice the calculation is performed by introducing cuts in $r = q_T/M$, with $r_{cut} \in [0.01\%, r_{max}]$ with r_{max} varying between 0.5% and 1%.

Predictions for differential distributions with different r_{cut} values

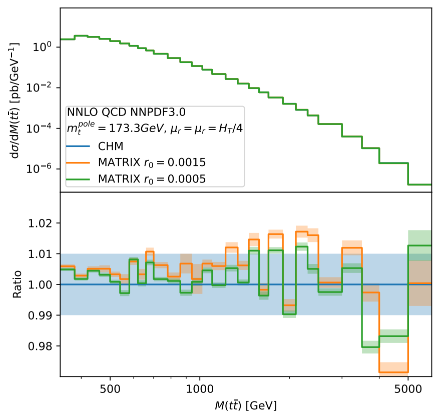

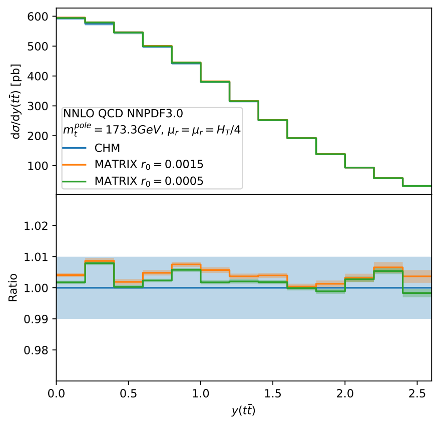

- ∗ In principle, the q_T-subtraction-based computation of (differential) cross-sections for finite r_{cut} introduces power corrections, which vanish in the limit $r_{cut} \to 0$.
- ∗ In practice, good agreement with the exact calculation (local) by Czakon, Heymes, Mitov (CHM) (at least considering their quoted 1% uncertainty).

Correlation between $m_t(m_t)$ and $\alpha_s(M_Z)$ in the old ABMP16 fit

from ABMP16 fit

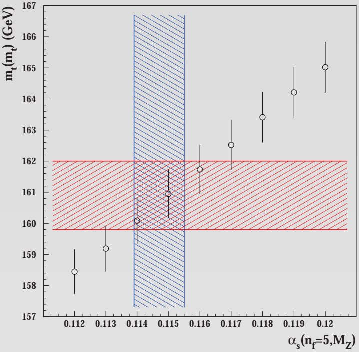

- Correlations between PDF $g(x)$, $\alpha_s(M_Z)$ and $m_t(m_t)$ follows from the factorization theorem.
- Fit of $m_t(m_t)$ at fixed $\alpha_s(M_Z)$ shows positive correlation between $\alpha_s(M_Z)$ value and $m_t(m_t)$.

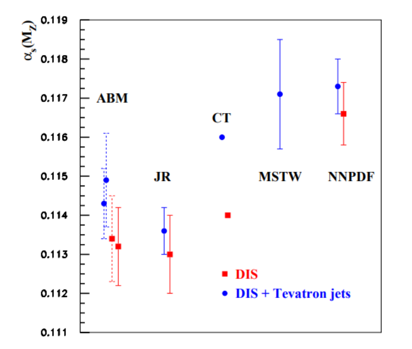

from S. Alekhin et al., PRD 89 (2014) 054028

∗ Differences in $\alpha_s(M_Z)$ between ABM and other PDF+$\alpha_s(M_Z)$ sets date back to 15 years...., in relation to:

- F_L treatment
- Effects of including/not including jet data from hadronic collisions (Tevatron and LHC)
- Effects of including/not including higher-twist corrections: an analysis without the latter brings back $\alpha_s(M_Z)$ at large values an analysis without the latter but with cuts on $Q^2 > 10$ GeV^2, $W^2 > 12.5$ GeV^2 lead to low $\alpha_s(M_Z)$ values.
- Other power corections to DIS: target mass corrections, due to finite nucleon mass

∗ Almost no impact of $t\bar{t} + X$ data on $\alpha_s(M_z)$: we would need to analyze $t\bar{t}j$ data.

ABMPtt fit: agreement with total inclusive cross-section data

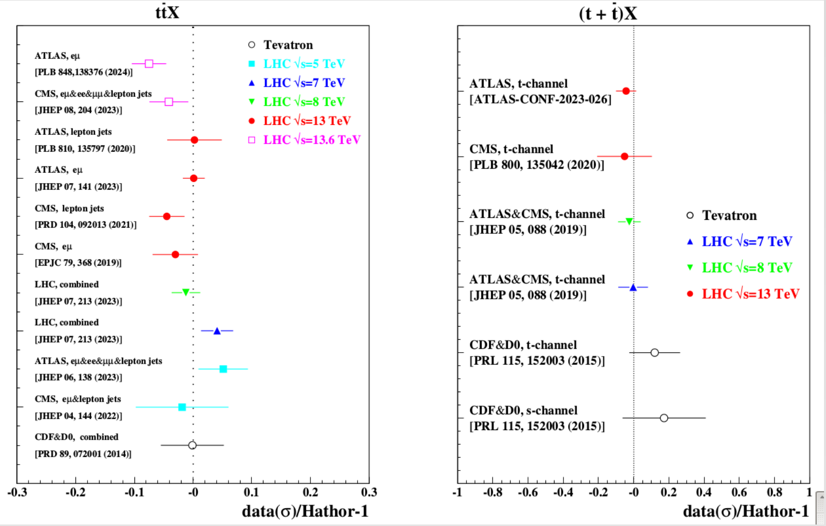

Good agreement with both $t\bar{t} + X$ and $(t + X)$ + $(\bar{t} + X)$ data (included in fit)